Article

Thermodynamic Feasibility Evaluation of Alkaline Thermal Treatment Process for Hydrogen Production and Carbon Capture from Biomass by Process Modeling

Yujung Jung and Sanghun Lee *

Department of Climate and Energy Systems Engineering, Ewha Womans University, Seoul 03760, Republic of Korea
* Correspondence: sanghun@ewha.ac.kr

Abstract: Hydrogen is attracting attention as a low-carbon fuel. In particular, economical hydrogen production technologies without carbon emissions are gaining increasing attention. Recently, alkaline thermal treatment (ATT) has been proposed to reduce carbon emissions by capturing carbon in its solid phase during hydrogen production. By adding an alkali catalyst to the conventional thermochemical hydrogen production reaction, ATT enables carbon capture through the reaction of an alkali catalyst and carbon. In this study, a thermodynamic feasibility evaluation was carried out, and the effects of the process conditions for ATT with wheat straw grass (WSG) as biomass were investigated using Aspen Plus software V12.1. First, an ATT process model was developed, and basic thermodynamic equilibrium compositions were obtained in various conditions. Then, the effects of the process parameters of the reactor temperature and the mass ratio of NaOH/WSG (alkali/biomass, A/B value) were analyzed. Finally, the product gas compositions, process efficiency, and amount of carbon capture were evaluated. The results showed that the ATT process could be an efficient hydrogen production process with carbon capture, and the optimal process conditions were a reactor temperature of 800 °C, an A/B value of three, and a flow rate of steam of 6.9×10^{-5} L/min. Under these conditions, the maximum efficiency and the amount of carbon dioxide captured were 56.9% and 28.41 mmol/g WSG, respectively.

Keywords: alkaline thermal treatment; hydrogen; biomass; process modeling; carbon capture

1. Introduction

The effects of climate change have been increasing due to greenhouse gas emissions, which are produced from fossil fuels. Thus, various scenarios are being analyzed around the world to achieve the goal of carbon neutrality. Research on new energy sources to replace fossil fuels is actively being conducted. These new energy sources should be easy to produce and transport as sustainable, clean energy without generating greenhouse gas emissions during their combustion.

Hydrogen is an energy source that satisfies this condition, and it could play an important role in decarbonizing to net zero CO_2 emissions by 2050 [1–5]. Hydrogen is used in various applications [6]. Compared to other fuels, hydrogen is good for use as a fuel because of its high energy efficiency [7]. For example, the energy from 9.5 kg of hydrogen is equal to the energy from 25 kg of gasoline [8]. In addition, hydrogen fuel cells can generate about five times more energy per unit of weight compared to lithium-ion batteries [9]. Because of these advantages, hydrogen fuel cells have a high energy density, allowing simple transportation [10]. In addition, hydrogen can be used as an energy carrier and storage medium [11]. Unlike other carbon-based fuels, hydrogen does not emit CO_2 during its combustion. Because of these advantages, hydrogen is widely used for power generation, vehicles, energy storage, and transportation. For power generation, hydrogen fuel cells have started to be used for small-to-medium-scale power plants [12]. Fuel-cell-based

ships, aircraft, and cars have been developed and commercialized in many countries [13]. Hydrogen-based energy storage systems (ESSs) are considered to improve the stability of power grids [14]. In addition, hydrogen imports across continents are being considered in some countries, such as Japan, Korea, and some European countries. The International Energy Agency (IEA) predicts that hydrogen demand will increase to 150 million tons in 2030. As of 2022, hydrogen usage was 43% of the oil refining sector and 56% of the industrial sector [15]. As hydrogen utilization methods become more diverse, hydrogen demand is expected to increase, and research related to hydrogen production is becoming more important.

Currently, there are three major methods of hydrogen production that are commercially available: coal gasification, methane reforming, and water electrolysis [16,17]. Since coal gasification and methane reforming are based on fossil fuels, they have limitations in terms of generating carbon dioxide, and water-electrolysis-produced hydrogen has the limitations of a high production cost and low efficiency [18]. Hydrogen production using fossil fuels can emit approximately 10.65 billion tons of CO_2 per year [19], which makes these conventional technologies unfavorable. On a commercial scale, hydrogen production in SMR, which accounts for about 40% of hydrogen production, can be more expensive than biomass gasification [20,21]. Hydrogen production using biomass is drawing attention for these reasons [22]. Biomass is abundant in nature and consumes CO_2 through photosynthesis as it grows, so it is both carbon-neutral and potentially carbon-negative, making it suitable as a green hydrogen production raw material. As a result, biomass thermochemical hydrogen production is drawing attention as a sustainable process [23–25]. However, the biomass steam gasification reaction, which is the most common method of hydrogen production from biomass, has the limitations of producing tar and several by-products, lowering the hydrogen purity. The conventional steam gasification hydrogen production process has a complex reaction path, and various by-products are produced in addition to hydrogen.

The alkaline thermal treatment (ATT) process resolves the above problems. The ATT process simplifies the reaction path by reacting alkali catalysts with biomass. Then, the sodium ions of the alkali catalyst used in the reaction react with CO_2, which is produced during gasification as a by-product of Na_2CO_3 (sodium carbonate). As a result, the ATT process has the advantages of suppressing CO_2 generation and reducing the energy required for hydrogen production by simplifying the reaction path. In addition, porous solid carbon can be obtained as a product of the ATT process, and it can be used in a wide range of applications including as adsorbents or electrode materials in wastewater treatment [19]. In this way, it has the advantages of both reducing carbon emissions and allowing by-products to be used in various ways compared to conventional gasification.

However, most previous studies have focused on the basic feasibility of the ATT process by selecting catalyst materials and finding suitable reaction conditions using a screening method [26–29]. Qi et al. used rice husk as the biomass to investigate a strategy for the co-production of porous carbon and high-purity hydrogen through the ATT process and reported optimal conditions of an alkali/rice husk mass ratio of 3:1 and a reaction temperature of 500 °C [27]. Doranehgard et al. studied a process using CaO to prevent tar formation and CO_2 emissions, which are major obstacles to hydrogen production [26]. Stonor et al. investigated the role of $CaOH_2$ as a catalyst to produce hydrogen with carbon capture using the ATT process and reported suppressed CO_2 formation with a low reaction temperature of 773 °C compared to other catalysts [28]. Ming Zhao et al. reported the ATT process with cellulosic biomass as a fuel for hydrogen production, and it showed high hydrogen yield at an elevated temperature [29].

To further evaluate the feasibility of the ATT process, a more comprehensive study in terms of thermodynamic equilibrium and process design should be conducted, in addition to simple chemical reaction testing. The purpose of this study was to investigate the effects of the reaction conditions on the ATT process based on thermodynamic equilibrium and reactor system modeling and simulation to calculate efficiency and amount of carbon

capture and to explore the optimal reaction conditions of the ATT process. To achieve the goal, we conducted a process modeling and simulation study on the ATT process utilizing Aspen Plus software V12.1, which is the most common chemical process modeling tool in the petrochemical industry. The process modeling was developed based on a thermodynamic-based Gibbs reactor and a field reactor based on experimental data. In each model, the changes in hydrogen production and gas compositions were explored according to the reactor temperature and the amount of catalyst. The effects of process conditions on the ATT process and carbon capturing during the reaction were discussed.

2. Modeling and Simulation

2.1. Hydrogen Production Process Modeling

For the ATT process, wheat straw grass (WSG) was used as the biomass. The material properties of WSG were obtained from the literature [30]. Ultimate and proximate analysis results are shown in Tables 1 and 2, respectively [30,31]. The WSG was mainly composed of carbon, hydrogen, and oxygen from the ultimate analysis. The basic process conditions of this study are shown in Table 3. To simulate the reaction of WSG, the catalyst and WSG were supplied together with feed. In this study, the ATT hydrogen production process was simulated in two ways: thermodynamic equilibrium-based and experimental-based. The thermodynamic equilibrium-based process simulation is shown in Figure 1a, and the experimental-based process is shown in Figure 1b. The following is a description of the process conditions for each component used in Aspen Plus. The drying processes proceeded in the same way, and the phase to be performed after the drying process is described separately for the two processes.

**Table 1.** Ultimate analysis of biomass WSG.

Element	Ultimate Analysis wt% (Dry Ash-Free Basis)	
C	49.0	
H	6.8	
O	44.2	[31]
N	0.0	

Table 2. Moisture, ash ratio, and proximate analysis of biomass WSG.

Type	Proximate Analysis wt%	
Moisture (wet basis)	2.3	
Ash (dry basis)	4.2	
FC (dry basis)	10.98	[30,31]
VM (dry basis)	82.12	

Table 3. Basic process conditions.

Variables	Basic Process Conditions (WSG Supply 250 mg/min)	
Reactor temperature	500 °C	
Alkali/Biomass mass ratio	3/1	[31]
Steam flow rates (mg/min)	5.75	
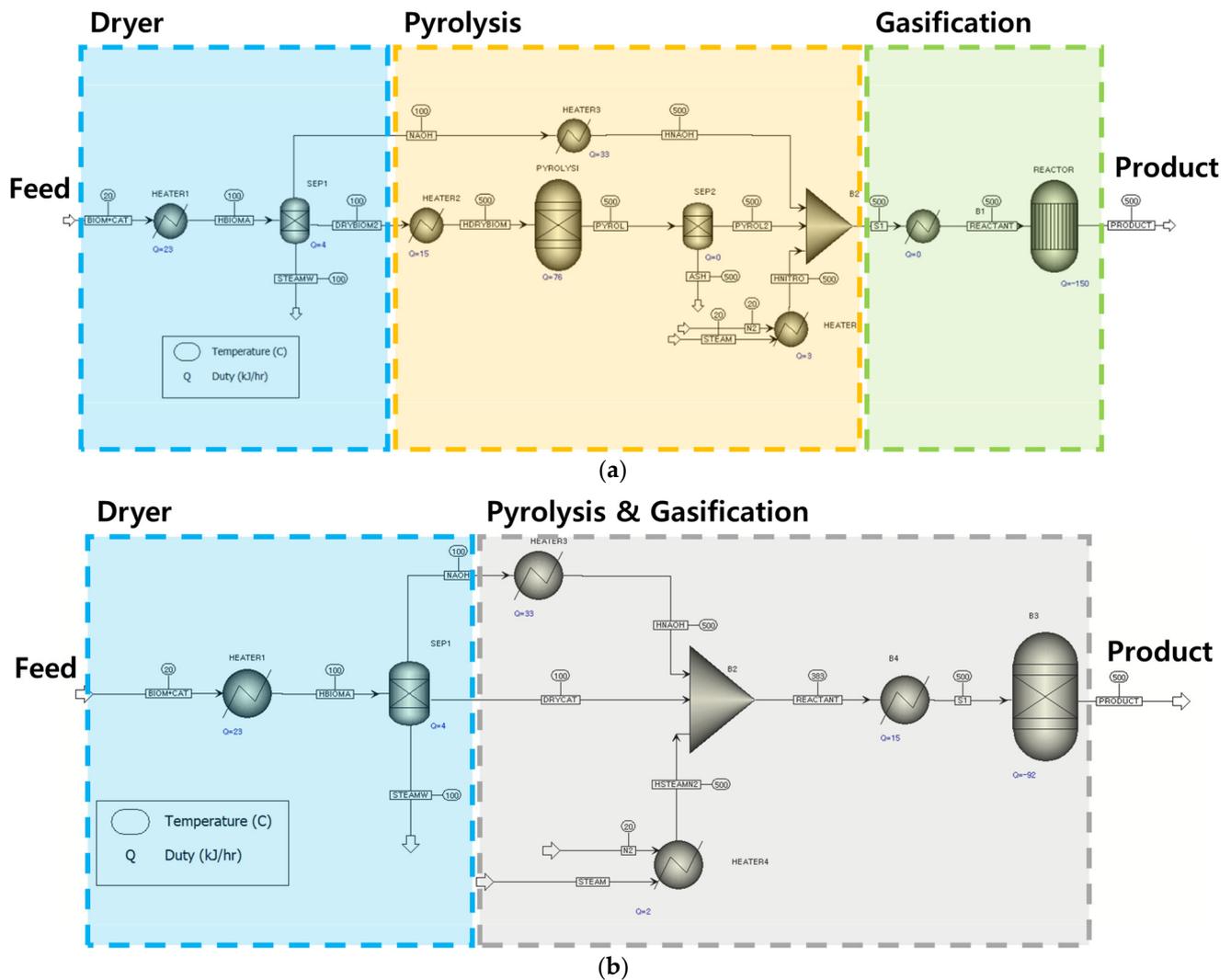
Figure 1. Schematic diagram of gasification modeling based on (**a**) thermodynamic equilibrium and (**b**) experiments.

For WSG to participate in the reaction, the dryer must evaporate the water in the catalyst solution. The dryer is designed as an RStoic reactor, and the temperature of the dryer was set to 100 °C. Wet WSG and NaOH solution (50 wt%) were supplied to the dryer at a flow rate of 250 mg/min and 750 mg/min, respectively, resulting in an alkali/biomass (A/B) ratio of 3. Evaporated water in the catalyst solution was removed through a separator of the dryer. Subsequent phases of pyrolysis and gasification processes were explored based on thermodynamic equilibrium and experimental-data-based modeling as follows.

2.1.1. Gasification Modeling Based on Thermodynamics

For thermodynamic modeling, the pyrolysis of WSG in a pyrolysis reactor was modeled using an RYield reactor. Since biomass WSG is a non-conventional material in the Aspen Plus software, thermochemical properties were not provided. Therefore, WSG pyrolysis was modeled based on the ultimate and proximate data. The pyrolysis temperature was assumed to be 500 °C. As a result, the WSG was decomposed into 49.0 wt% carbon, 6.8 wt% hydrogen, 44.2 wt% oxygen, and 4.2 wt% ash. The decomposed ash was removed through a separator.

Then, gasification of the WSG was modeled with an RGibbs reactor. Carbon, hydrogen, and oxygen obtained from the RYield reactor reacted with dry NaOH, and N_2 and water were supplied to the reactor to produce hydrogen in the RGibbs reactor at a temperature

of 500 °C. Then, the final gas composition of the outlet gas from the RGibbs reactor was analyzed to investigate the product gases of the ATT process.

2.1.2. Gasification Modeling Based on Literature Data

In addition to the thermodynamics equilibrium, the following modeling was also performed based on the previously reported experimental results [31]. The results are presented in Tables 4 and 5 below. For this modeling, the experimental results were used as process conditions, and a single RYield reactor was used for modeling both the pyrolysis and gasification reactors. Using this modeling, the ATT process was simulated to compare the modeling based on thermodynamics and experimental data. Since only 500 °C data were complete, comparisons between processes were performed only for 500 °C.

Table 4. Yields from the ATT of wet WSG at temperatures from 300 to 600 °C based on experiments (A/B mass ratio = 3).

	300 °C	400 °C	500 °C	600 °C
H_2 (mmol/g WSG)	24.174	29.652	37.262	37.913
CH_4 (mmol/g WSG)	0.083	5.222	5.253	7.250
C_2H_6 (mmol/g WSG)	0.002	0.001	0.001	0.140
CO_2 (mmol/g WSG)	0.079	0.103	0.252	0.448
NaOH (mmol/g WSG)	Unknown	Unknown	58.303	Unknown
Na_2CO_3 (mmol/g WSG)	Unknown	Unknown	8.570	Unknown

Table 5. Yields from the ATT of wet WSG with A/B mass ratio varied from 0 to 5 based on experiments (reaction temperature = 500 °C).

	0:1	1:1	2:1	3:1	5:1
H_2 (mmol/g WSG)	3.191	15.837	29.416	37.262	36.342
CH_4 (mmol/g WSG)	0	0	1.477	5.253	5.036
C_2H_6 (mmol/g WSG)	0.002	0.253	0.001	0.001	0
CO_2 (mmol/g WSG)	3.310	2.046	0.948	0.252	0.107

2.2. Efficiency Calculation

To calculate the efficiency of each model, heat input calculated with Aspen Plus software was used. The thermal efficiency was calculated for the process simulated under the basic process conditions, and efficiency was measured as system efficiency, cold gas efficiency (CGE), and gas yield (GY). CGE only considers the produced gas heating value [32]. Since WSG was supplied at 250 mg/min, the input heating value in all models is as below. Because only the higher heating value (HHV) has been reported for the biomass composition in this study, HHV was used for the efficiency calculation and comparison [33]. The HHV of WSG is 17.988 MJ/kg on a dry basis [33]. Therefore, the heating value of 250 mg of WSG is 17.988/4 kJ = 4.497 kJ. The HHV of H_2 is 142 MJ/kg [34]. An efficiency calculation was performed according to the following equation.

System efficiency: H_2 HHV × mass of H_2/(HHV for 250 mg WSG + heat required)

CGE: H_2 HHV × mass of H_2/(HHV for 250 mg WSG)

GY: Mass of (H_2 + CH_4 + CO_2 + C_2H_6 + O_2)

2.3. Sensitivity Analysis

2.3.1. Gasification Modeling Based on Thermodynamics

Three variables were selected for the sensitivity analysis of thermodynamics modeling: the temperature of the reactor, the A/B ratio, and the flow rate of steam. First, the effects of RGibbs reactor temperature were analyzed. In the hydrogen production process, the temperature of the reactor greatly affects the product gas composition. Therefore, sensitivity analysis according to the temperature of the RGibbs reactor was conducted from 200 °C to 1200 °C, and the changes in hydrogen, CO_2, CH_4, and C_2H_6 were compared. Second, the effects of A/B ratio were analyzed. In the ATT process, as Na^+ ions of NaOH can capture carbon and prevent greenhouse gas emissions, the effects of NaOH mass were investigated to find a suitable amount of NaOH for the ATT process. Sensitivity analysis was conducted for A/B values from 1 to 5 to confirm the changes in hydrogen production and CO_2 captured during the ATT process according to the A/B value. Third, hydrogen production was analyzed with different flow rates of steam. The amount of steam can change the product gas composition and process efficiency significantly. Therefore, a sensitivity analysis was conducted using a four times greater feed rate of 23 mg/min.

2.3.2. Gasification Modeling Based on Literature Data

The sensitivity analysis based on the results of experiments involved an analysis of the thermal efficiency obtained in each condition because it sets a fixed amount of production based on the results of the experiments. Thermal efficiencies for the different temperatures and catalyst amounts were analyzed as an important index in the efficiency of the process.

3. Results and Discussion

3.1. Process Modeling Based on Thermodynamic Equilibrium

3.1.1. Results Based on Basic Conditions

Figure 2 and Table 6 show the yield of each product of the reaction obtained by the model according to the basic process conditions of Table 3. For 1 g of WSG, 42.99 mmol/min of hydrogen was produced and 28.41 mmol/min of Na_2CO_3 was produced. Na_2CO_3 is a residue of the reaction of the catalyst NaOH with CO_2, in which carbon capture can be conducted as follows:

$$2NaOH + CO_2 \rightarrow Na_2CO_3 + H_2O$$
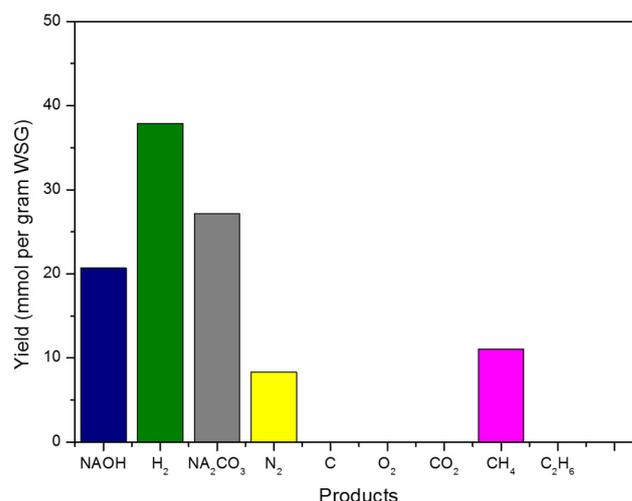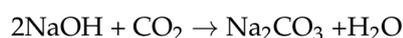
Figure 2. Yield of ATT H_2 production based on thermodynamics (reaction temperature = 500 °C, A/B mass ratio = 3).

The molar ratio of the CO_2 captured to the production of Na_2CO_3 is 1:1. Therefore, as Na_2CO_3 was produced at 28.41 mmol/min per 1 g of WSG, 28.41 of CO_2 mmol/min was

captured. Also, because NaOH was supplied at 75 mmol/g WSG, the remaining NaOH was 18.18 mmol/g WSG.

Table 6. Yields from the ATT of wet WSG based on thermodynamic equilibrium (reaction temperature = 500 °C, A/B mass ratio = 3).

Products	Yields (mmol/g WSG)
H_2	37.88
CH_4	11.05
C_2H_6	4.53×10^{-5}
CO_2	0
NaOH	18.18
Na_2CO_3	28.41

3.1.2. Sensitivity Analysis for ATT Based on Thermodynamic Equilibrium

Effects of RGibbs Reactor Temperature

The results of the sensitivity analysis with a reactor temperature from 200 °C to 1200 °C are shown in Figure 3. The product yields of the reaction and the system efficiencies were obtained based on the thermodynamics equilibrium. The number of moles of hydrogen produced greatly increased between 600 °C and 800 °C but showed little change at higher temperatures. CO_2 showed a result close to zero even at low temperatures. At the same time, Na_2CO_3 showed a constant value regardless of temperature. Thus, CO_2 reacted quickly with Na ions to produce Na_2CO_3 immediately after CO_2 was generated based on the rapid reaction of alkali catalysts with CO_2 [35]. A relationship between the increase in hydrogen production and the decrease in methane was observed. Since the amount of hydrogen produced increased by twice as much as the amount of methane production decreased, we concluded that methane decomposed into carbon and hydrogen as the temperature increased, thereby increasing the amounts of hydrogen and carbon. Therefore, conducting the reaction at a temperature higher than that of methane decomposition can provide good results. While increasing the temperature aids in hydrogen production, if the temperature is too high, a lot of energy is required for the reaction, and costs may increase due to the need for a material that can withstand high temperatures. Accordingly, we concluded that the optimum temperature is 800 °C.
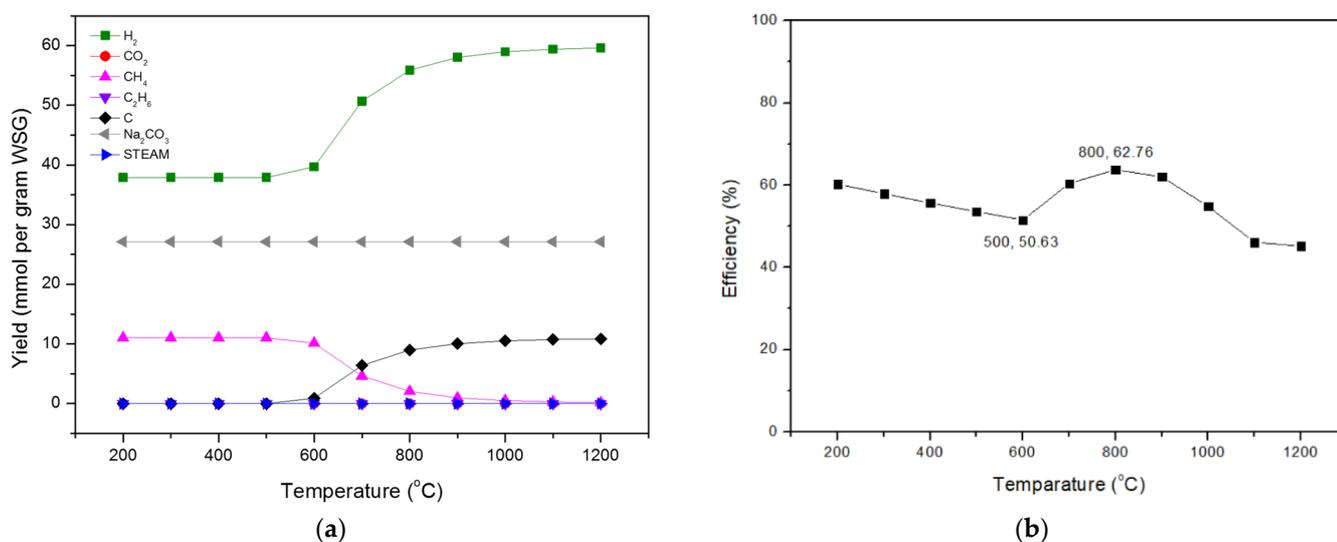
Figure 3. (**a**) Effects of reaction temperature yield and (**b**) system efficiency as a function of temperature.

Effects of Alkali/Biomass Mass Ratio

The number of moles of gas produced per 1 g of WSG according to the alkali/biomass mass ratio and system efficiency based on the thermodynamics equilibrium is presented in Figure 4. The amount of Na_2CO_3 produced increased rapidly up to an A/B value of 2 and then changed little with further temperature increase. Amounts of carbon, CO_2, and CH_4 decreased above an A/B ratio of 2 because the substances are involved in the synthesis of Na_2CO_3. Overall, CO_2 production decreased and Na_2CO_3 production increased as the NaOH catalyst supply increased, which implies that NaOH captures CO_2. An increase in alkali catalyst supply can also increase hydrogen production and CO_2 capture. However, an increase in the supply of the alkali catalyst may lead to an increase in cost. Therefore, an optimal A/B ratio of 3 was used here.
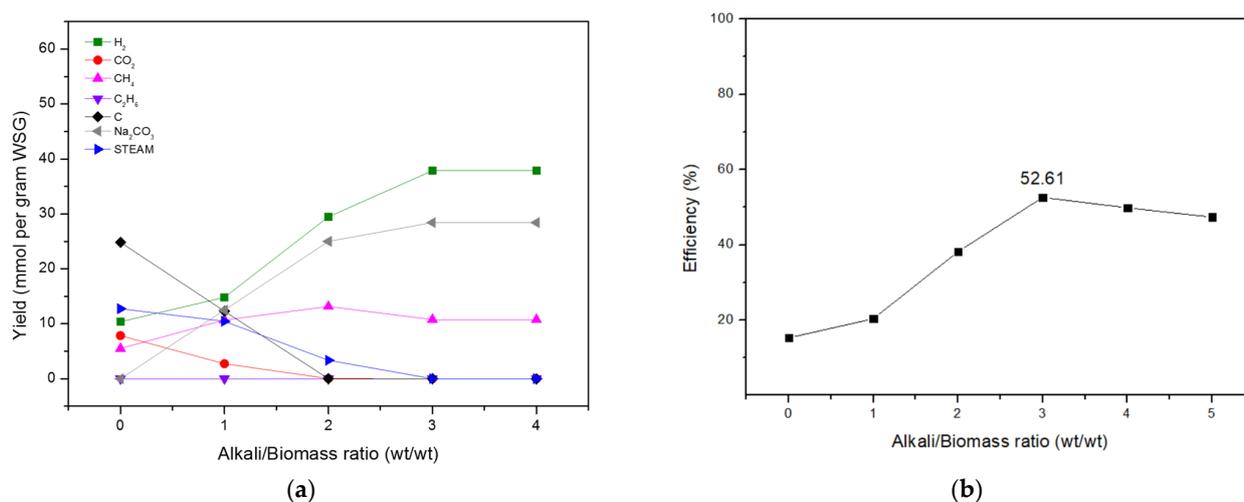

Figure 4. Effects of A/B ratio on (**a**) yield and (**b**) system efficiency.

Effects of Steam Flow Rate

The product yields of the reaction and system efficiencies according to the amount of steam are shown in Figure 5. As the steam participating in the reaction increases, the amount of hydrogen produced increases. This can be attributed to the effect of hydrogen production by the decomposition of steam. Accordingly, since the amount of hydrogen produced increases as more water is involved in the reaction, supplying as much water as possible can be a good option. However, since increasing the water supply increases water cost and decreases the efficiency of the reaction, a balance is appropriate.
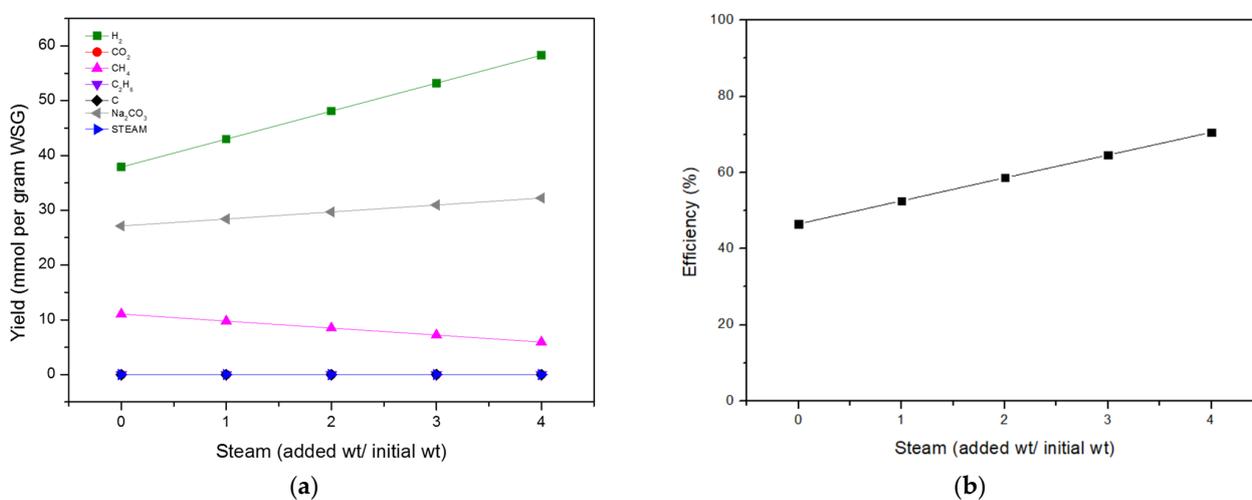

Figure 5. Effects of steam rate on (**a**) yield and (**b**) system efficiency of steam addition.

3.2. Process Modeling Based on Experimental Data

Process simulation can be used in numerous ways by changing simulation conditions. However, the experimental results are limited because it is difficult to conduct experiments for all conditions. As shown in Table 7 and Figure 6, the product yields obtained from the process modeling based on the experimental data revealed differences from the thermodynamic-based model shown in Figure 2. The amount of hydrogen produced was similar, but a significantly smaller amount of Na_2CO_3 was produced in the experiment-based simulation.

Table 7. Yields from the ATT of wet WSG based on experiments (reaction temperature = 500 °C, A/B mass ratio = 3).

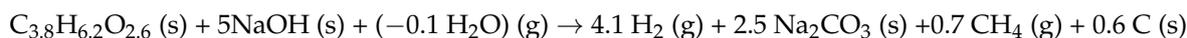| Products	Yields (mmol/g WSG)
H_2	37.262
CH_4	5.253
C_2H_6	0.001
CO_2	0.252
NaOH	58.303
Na_2CO_3	8.570
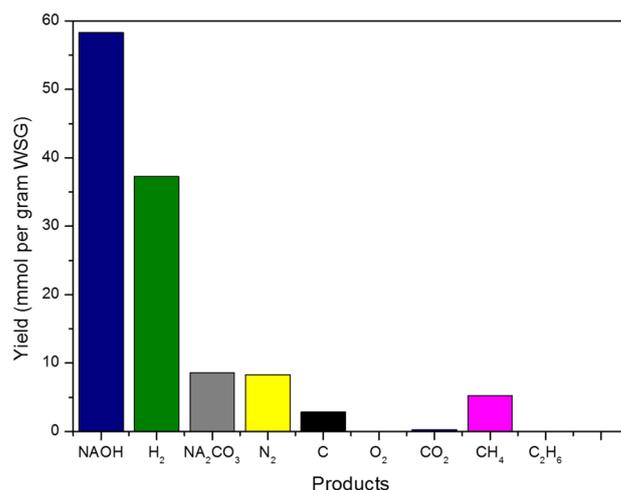
Figure 6. Yield of ATT H_2 production based on experiments.

The following are possible reasons for the difference between simulation and experiment results. First, the reaction could not achieve the thermodynamics equilibrium demonstrated in the experiments. The experiment was conducted for a fixed time of 3 h at the reaction temperature [31]. By fixing the reaction temperature, a fair comparison of the effects of reaction temperature was possible; however, the completeness of the reaction could not be ensured. Second, the smaller amount of CO_2 produced from the biomass may be due to changes in reaction completeness. In the simulation thermodynamics, all the carbon was assumed to be converted to gas phase species; a carbon-containing solid residue was observed in the experiments. As a result, NaOH could react with a small amount of CO_2, resulting in a larger amount of remaining NaOH and a smaller amount of Na_2CO_3.

3.3. Comparisons of Gasification Results: Stoichiometric Equation, Thermodynamic Equilibrium, and Literature Data

3.3.1. Efficiency Calculation of a Stoichiometric Model

The chemical reaction formula representing the general ATT reaction presented in the literature is as follows [31]:

$$C_{3.8}H_{6.2}O_{2.6} \text{ (s)} + 5NaOH \text{ (s)} + (-0.1 \text{ } H_2O) \text{ (g)} \rightarrow 4.1 \text{ } H_2 \text{ (g)} + 2.5 \text{ } Na_2CO_3 \text{ (s)} +0.7 \text{ } CH_4 \text{ (g)} + 0.6 \text{ } C \text{ (s)}$$

The product yield was calculated based on the above reaction equation as shown in Table 8.

Table 8. Calculated yields from the ATT of wet WSG (reaction temperature = 500 °C, A/B mass ratio = 3).

Products	Yields (at 500 °C)
H_2 (mmol/g WSG)	42.90
Na_2CO_3 (mmol/g WSG)	26.37
CH_4 (mmol/g WSG)	7.364
C (mmol/g WSG)	6.323
CO_2 (mmol/g WSG)	0.1895
C_2H_6 (mmol/g WSG)	0.1380

The heat required in the stoichiometric model is 77 kJ/h (1.283 kJ/min). Also, because 10.73 mmol (=21.45 mg) of hydrogen was produced per 250 mg WSG in 1 min, it can release 142 kJ/g × 21.45 mg = 3.046 kJ according to the HHV of hydrogen. As mentioned in Section 2.2, the heating value of 250 mg of WSG is assumed to be 17.988/4 kJ = 4.497 kJ.

System efficiency: 3.046/(4.497 + 1.283) = 52.40%

CGE: 3.046/4.497 = 67.73%

GY: 0.2171 g/1 g WSG

3.3.2. Efficiency Calculation of a Thermodynamic-based Model

The heat required in the thermodynamic-based model was 143 kJ/h from process modeling. Therefore, the amount of heat to be supplied per minute was 143/60 kJ/min = 2.383 kJ. As 9.47 mmol = 18.94 mg of hydrogen was produced per 250 mg WSG in 1 min, it can release 142 kJ/g/1000 × 18.94 = 2.689 kJ of energy according to the HHV of hydrogen.

System efficiency: 2.689/(4.497 + 2.383) = 39.08%

CGE: 2.689/4.497 = 59.80%

GY: 0.2435 g/1 g WSG

3.3.3. Efficiency Calculation of the Experiment-based Model

The heat required in the thermodynamic-based model was 77 kJ/h. Therefore, the amount of heat to be supplied per minute was 77/60 kJ/min = 1.283 kJ. Since 9.316 mmol = 18.63 mg of hydrogen was produced per 250 mg WSG in 1 min, 142 kJ/g /1000 × 18.63 = 2.645 kJ energy was released according to the HHV of hydrogen.

Efficiency: 2.645/(4.497 + 1.283) = 45.76%

CGE: 2.645/4.497 = 58.82%

GY: 0.1705 g/1 g WSG

Table 9 shows a comparison of the results for stoichiometric, thermodynamic, and experiment-based modeling. Through process simulation, we determined the amount of heat required, system efficiency, and CGE for each of the three models. The model with the worst system efficiency was the thermodynamic-based model, likely because the heat required for modeling was included in the system efficiency calculation. The

thermodynamic-based model provides a lot of heat because all reactions reach thermodynamic equilibrium. Additionally, since the thermodynamic-based model produced hydrogen through pyrolysis, the heat consumed in the pyrolysis process was also included. The highest efficiency was with the model based on stoichiometry, which considers only the quantitative relationship of the reactants, ignoring both thermodynamic and experimental limitations. Therefore, good efficiency was achieved because more hydrogen was produced and less heat was supplied. In comparison, CGE depends only on the supplied reactants and the amount of hydrogen produced and was highest in the stoichiometry-based model and similar in the thermodynamic- and experiment-based models. In the case of GY, the thermodynamic-based simulation showed the largest value, as the experiment did not reach the thermodynamic equilibrium.

Table 9. Comparison of the results of all models.

	Heat Required (kJ/h)	H_2 Production (mmol/g WSG)	System Efficiency (%)	CGE (%)	GY (g/1 g WSG)
Stoichiometry	77	42.90	52.40	67.73	0.2171
Thermodynamic	143	37.88	39.08	59.80	0.2537
Experiment	77	37.26	45.76	58.82	0.1705

3.4. Implications and Limitations

In this study, a comprehensive simulation of the recently proposed ATT process was conducted using Aspen Plus software. We reached three main conclusions. First, thermodynamic modeling was performed to analyze the characteristics of the ATT reaction depending on the process conditions. Suggesting optimal process conditions based on thermodynamic equilibrium provided an increased understanding of the characteristics of the ATT reaction, and these can be used to determine the process conditions in follow-up studies. Second, by simulating the process, we predicted the amounts of hydrogen production and carbon capture that could be obtained, confirming the feasibility of the ATT process for hydrogen production and carbon capture. Additionally, by comparing and analyzing simulations based on thermodynamic equilibrium and experimental results, we quantitatively demonstrated that the ATT experiment did not achieve thermodynamic equilibrium, indicating a potential for improved hydrogen production and carbon capture through the development of new catalyst materials, structures, and reactor designs.

The ATT process is in its initial research stage and has the following limitations. Firstly, the scope of published research is limited. This made it difficult to compare and analyze our results. Secondly, we were unable to conduct comparative analysis on various biomasses of rice husk, cellulosic biomass, straw, and celery or catalyst materials of KOH, CaO, and Ca(OH)$_2$ This is because research on the ATT process is still in the early stage. Lastly, optimal process and hydrogen production conditions and detailed economic comparative analysis studies must be performed for the commercialization of the ATT process. Based on this, the strengths and limitations of ATT must be compared to those of existing hydrogen production and carbon capture technologies. In addition, both the economic aspect and the amount of greenhouse gases emitted during hydrogen production are attracting attention due to decarbonization [36]. However, since the ATT process is in the initial stages of development and the related literature is scarce, discussing this aspect was challenging. Therefore, we expect that more detailed comparative analyses will be possible with continuing research.

4. Conclusions

In this study, the hydrogen production reaction using the ATT process with WSG was simulated through Aspen Plus. To commercialize the ATT process technology, an approach from the process unit is required along with the results obtained from experiments. In Aspen Plus, the process was simulated using certain variables, and the thermodynamically

calculated results were derived. Under the basic conditions of the process based on thermodynamic equilibrium, hydrogen was produced at 37.88 mmol/g WSG, and carbon dioxide was captured at 28.41 mmol/min. As a result of hydrogen production through ATT, the production of hydrogen was 1.75 times higher than in a previous study [33], which showed a production rate of 21.6 mmol/min per 1 g of WSG. In other words, the ATT process has strengths both in suppressing greenhouse gas emissions and in producing high-purity hydrogen if the conditions are optimized and proper catalysts are developed. Based on the sensitivity analysis, the optimum temperature of the reactor, the amount of alkali, and the amount of steam based on efficiency were 800 °C, 3:1, and the maximum amount of steam, respectively. Under these conditions, the maximum efficiency was 56.9%. In addition, the maximum carbon dioxide capture was 28.41 mmol/g WSG. Overall, we conducted a comprehensive study on the ATT process, which is still in its early stage. It is expected that this work will contribute to the development and commercialization of the ATT process.

Author Contributions: Conceptualization, Y.J. and S.L.; methodology, Y.J. and S.L.; software, Y.J.; validation, Y.J. and S.L.; formal analysis, Y.J.; investigation, Y.J. and S.L.; resources, Y.J. and S.L.; data curation, Y.J.; writing—original draft preparation, Y.J.; writing—review and editing, S.L.; visualization, Y.J.; supervision, S.L.; project administration, S.L.; funding acquisition, S.L. All authors have read and agreed to the published version of the manuscript.

Data Availability Statement: The raw data supporting the conclusions of this article will be made available by the authors on request.

Conflicts of Interest: The authors declare no conflict of interest.

References

1. Masson-Delmotte, V.; Zhai, P.; Pörtner, H.; Roberts, D.; Skea, J.; Shukla, P.; Pirani, A.; Moufouma-Okia, W.; Péan, C.; Pidcock, R. Global Warming of 1.5 °C. An IPCC Special Report on the Impacts of Global Warming of 1.5 °C above Pre-industrial Levels and Related Global Greenhouse Gas Emission Pathways, in the Context of Strengthening the Global Response to the Threat of Climate Change, Sustainable Development, and Efforts to Eradicate Poverty. Intergovernmental Panel on Climate Change (IPCC). 2018. Available online: https://www.ipcc.ch/sr15/ (accessed on 1 October 2023).
2. Jang, Y.-H.; Lee, S.; Shin, H.Y.; Bae, J. Development and evaluation of a 3-cell stack of metal-based solid oxide fuel cells fabricated via a sinter-joining method for auxiliary power unit applications. *Int. J. Hydrogen Energy* **2018**, *43*, 16215–16229. [CrossRef]
3. Lee, H.; Lee, S. Economic Analysis on Hydrogen Pipeline Infrastructure Establishment Scenarios: Case Study of South Korea. *Energies* **2022**, *15*, 6824. [CrossRef]
4. Lee, S.; Lee, K.; Lee, J.; Lee, J.; Kim, T.; Bae, J. Evaluation of Electrolyte Materials of Gd-and Ce-Doped Scandia-Stabilized Zirconia and Yb-and Bi-Doped Gadolinium-Doped Ceria for Highly Durable Solid Oxide Fuel Cells. *Int. J. Precis. Eng. Manuf.-Green Technol.* **2023**, 1–12. [CrossRef]
5. Park, H.; Kim, K.; Yu, M.; Yun, Z.; Lee, S. Economic analysis of the circular economy based on waste plastic pyrolysis oil: A case of the university campus. *Environ. Dev. Sustain.* **2023**, *26*, 6293–6313. [CrossRef]
6. Ramachandran, R.; Menon, R.K. An overview of industrial uses of hydrogen. *Int. J. Hydrog. Energy* **1998**, *23*, 593–598. [CrossRef]
7. Furusawa, Y.; Taguchi, H.; Ismail, S.N.; Thangavel, S.; Matsuoka, K.; Fushimi, C. Estimation of cold gas efficiency and reactor size of low-temperature gasifier for advanced-integrated coal gasification combined cycle systems. *Fuel Process Technol.* **2019**, *193*, 304–316. [CrossRef]
8. Ultanir, M. Hidrojenin yakıt olarak kullanımı ve özellikleri. In Proceedings of the Çevre-Enerji Kongresi, TMMOB Makine Mühendisleri Odası, Ankara, Turkey, 5–7 June 1997; pp. 195–315.
9. Oh, G.; Jang, J.Y.; Ra, H.W.; Seo, M.W.; Mun, T.Y.; Lee, J.-G.; Yoon, S.J. Gasification of Coal and Torrefied Biomass Mixture. *Trans. Korean Hydrog. New Energy Soc.* **2017**, *28*, 190–199. [CrossRef]
10. Felseghi, R.-A.; Carcadea, E.; Raboaca, M.S.; Trufin, C.N.; Filote, C. Hydrogen fuel cell technology for the sustainable future of stationary applications. *Energies* **2019**, *12*, 4593. [CrossRef]
11. Ishaq, H.; Dincer, I.; Crawford, C. A review on hydrogen production and utilization: Challenges and opportunities. *Int. J. Hydrog. Energy* **2022**, *47*, 26238–26264. [CrossRef]

12. Cook, B. Introduction to fuel cells and hydrogen technology. *Eng. Sci. Educ. J.* **2002**, *11*, 205–216. [CrossRef]

13. Roh, G.; Kim, H.; Jeon, H.; Yoon, K. Fuel consumption and CO_2 emission reductions of ships powered by a fuel-cell-based hybrid power source. *J. Mar. Sci. Eng.* **2019**, *7*, 230. [CrossRef]

14. Dutta, S. A review on production, storage of hydrogen and its utilization as an energy resource. *J. Ind. Eng. Chem.* **2014**, *20*, 1148–1156. [CrossRef]

15. IEA. *Global Hydrogen Review 2023*; IEA: Paris, France, 2023. Available online: https://www.iea.org/reports/global-hydrogen-review-2023 (accessed on 1 October 2023).

16. Soltani, S.M.; Lahiri, A.; Bahzad, H.; Clough, P.; Gorbounov, M.; Yan, Y. Sorption-enhanced steam methane reforming for combined CO_2 capture and hydrogen production: A state-of-the-art review. *Carbon Capture Sci. Technol.* **2021**, *1*, 100003. [CrossRef]

17. Sobolyeva, T. On the Microstructure of PEM Fuel Cell Catalyst Layers. Ph.D. Thesis, Simon Fraser University, Burnaby, BC, Canada, 2010.

18. Younas, M.; Shafique, S.; Hafeez, A.; Javed, F.; Rehman, F. An overview of hydrogen production: Current status, potential, and challenges. *Fuel* **2022**, *316*, 123317. [CrossRef]

19. Kalinci, Y.; Hepbasli, A.; Dincer, I. Biomass-based hydrogen production: A review and analysis. *Int. J. Hydrog. Energy* **2009**, *34*, 8799–8817. [CrossRef]

20. Franchi, G.; Capocelli, M.; De Falco, M.; Piemonte, V.; Barba, D. Hydrogen production via steam reforming: A critical analysis of MR and RMM technologies. *Membranes* **2020**, *10*, 10. [CrossRef]

21. Bocci, E.; Di Carlo, A.; Vecchione, L.; Villarini, M.; De Falco, M.; Dell'Era, A. Technical-economic analysis of an innovative cogenerative small scale biomass gasification power plant. In Proceedings of the Computational Science and Its Applications–ICCSA 2013: 13th International Conference, Ho Chi Minh City, Vietnam, 24–27 June 2013; pp. 256–270.

22. Rosa, L.; Mazzotti, M. Potential for hydrogen production from sustainable biomass with carbon capture and storage. *Renew Sustain. Energy Rev.* **2022**, *157*, 112123. [CrossRef]

23. Chandra, R.; Takeuchi, H.; Hasegawa, T.; Kumar, R. Improving biodegradability and biogas production of wheat straw substrates using sodium hydroxide and hydrothermal pretreatments. *Energy* **2012**, *43*, 273–282. [CrossRef]

24. Mani, T.; Murugan, P.; Abedi, J.; Mahinpey, N. Pyrolysis of wheat straw in a thermogravimetric analyzer: Effect of particle size and heating rate on devolatilization and estimation of global kinetics. *Chem. Eng. Res. Des.* **2010**, *88*, 952–958. [CrossRef]

25. Babatabar, M.A.; Saidi, M. Hydrogen production via integrated configuration of steam gasification process of biomass and water-gas shift reaction: Process simulation and optimization. *Int. J. Energy Res.* **2021**, *45*, 19378–19394. [CrossRef]

26. Doranehgard, M.H.; Samadyar, H.; Mesbah, M.; Haratipour, P.; Samiezade, S. High-purity hydrogen production with in situ CO_2 capture based on biomass gasification. *Fuel* **2017**, *202*, 29–35. [CrossRef]

27. Qi, P.; Su, Y.; Zhang, S.; Jiang, M.; Sun, X.; Shi, L.; Xiong, Y. An innovative strategy on co-production of porous carbon and high purity hydrogen by alkaline thermal treatment of rice husk. *Int. J. Hydrog. Energy* **2022**, *47*, 23151–23164. [CrossRef]

28. Stonor, M.R.; Ouassil, N.; Chen, J.G.; Park, A.-H.A. Investigation of the role of $Ca(OH)_2$ in the catalytic Alkaline Thermal Treatment of cellulose to produce H2 with integrated carbon capture. *J. Energy Chem.* **2017**, *26*, 984–1000. [CrossRef]

29. Zhao, M.; Cui, X.; Ji, G.; Zhou, H.; Vuppaladadiyam, A.K.; Zhao, X. Alkaline thermal treatment of cellulosic biomass for H_2 production using Ca-based bifunctional materials. *ACS Sustain. Chem. Eng.* **2018**, *7*, 1202–1209. [CrossRef]

30. Channiwala, S.; Parikh, P. A unified correlation for estimating HHV of solid, liquid and gaseous fuels. *Fuel* **2002**, *81*, 1051–1063. [CrossRef]

31. Zhou, H.; Park, A.-H.A. Bio-energy with carbon capture and storage via alkaline thermal Treatment: Production of high purity H_2 from wet wheat straw grass with CO_2 capture. *Appl. Energy* **2020**, *264*, 114675. [CrossRef]

32. Kirsanovs, V.; Blumberga, D.; Veidenbergs, I.; Rochas, C.; Vigants, E.; Vigants, G. Experimental investigation of downdraft gasifier at various conditions. *Energy Procedia* **2017**, *128*, 332–338. [CrossRef]

33. Waheed, Q.M.; Williams, P.T. Hydrogen production from high temperature pyrolysis/steam reforming of waste biomass: Rice husk, sugar cane bagasse, and wheat straw. *Energy Fuels* **2013**, *27*, 6695–6704. [CrossRef]

34. Kayfeci, M.; Keçebaş, A.; Bayat, M. Hydrogen production. In *Solar Hydrogen Production*; Elsevier: Amsterdam, The Netherlands, 2019; pp. 45–83.

35. Pan, S.-Y.; Chang, E.; Chiang, P.-C. CO_2 capture by accelerated carbonation of alkaline wastes: A review on its principles and applications. *Aerosol Air Qual. Res.* **2012**, *12*, 770–791. [CrossRef]

36. Li, J.; Cheng, W. Comparative life cycle energy consumption, carbon emissions and economic costs of hydrogen production from coke oven gas and coal gasification. *Int. J. Hydrog. Energy* **2020**, *45*, 27979–27993. [CrossRef]